Artificial Neural Network Based Identification of Multi-Operating-Point Impedance Model

Zhang, Mengfan; Wang, Xiongfei; Yang, Dongsheng; Christensen, Mads Graesboll

Published in:
IEEE Transactions on Power Electronics

DOI (link to publication from Publisher):
10.1109/TPEL.2020.3012136

Publication date:
2021

Document Version
Accepted author manuscript, peer reviewed version

IEEE POWER ELECTRONICS REGULAR PAPER/LETTER/CORRESPONDENCE

Artificial Neural Network based Identification of Multi-Operating-Point Impedance Model

Mengfan Zhang, *Student Member, IEEE*, Xiongfei Wang, *Senior Member*, *IEEE*, Dongsheng Yang, *Senior Member*, *IEEE* and Mads Græsbøll Christensen, *Senior Member*, *IEEE*

***Abstract*—The black-box impedance model of voltage source inverters (VSIs) can be measured at their terminals without access to internal control details, which greatly facilitate the analysis of inverter-grid interactions. However, the impedance model of VSI is dependent on its operating point and can have different profiles when the operating point is changed. This letter proposes a method for identifying the impedance model of VSI under a wide range of operating points. The approach is based on the artificial neural network (ANN), where a general framework for applying the ANN to identify the VSI impedance is established. The effectiveness of the ANN-based method is validated with the analytical impedance models.**

I. Introduction

In recent years, the massive use of voltage-source inverters (VSIs) makes the power system more flexible, sustainable and efficient, yet it also imposes new challenges to the grid stability [1]. The impedance-based modeling and analysis of VSIs have been increasingly used to address the grid-VSI interactions [2]. A prominent feature of this approach is that the impedance of VSI can be directly measured at its terminal without the prior knowledge of internal control systems, which enables a 'black-box' modeling and analysis. However, in practical applications, the impedance model of VSI can be changed with the operating point of the system, due to the nonlinear control dynamics of VSIs, e.g., the Phase-Locked Loop (PLL), the power control and the dc-link voltage control loops [3]. Hence, it is hard to screen the worst scenarios with the impedance measured from a single operating point of the system.

Considering the operating-point dependence, a large-signal impedance model is reported in [4], where the operating-point variation is translated into an impedance model as a function of the amplitude of the perturbation signal. Hence, it is an indirect representation of the converter impedance at different operating points. An alternative way is to derive the polytopic model for VSIs or dc-dc converters [5], [6], where the identified small-signal models at multiple operating points are combined with weighting functions, and thus a multi-operating-point impedance model can be obtained for predicting the impedance at different operating points, yet its accuracy depends on the number of small-signal models (operating points) combined in the polytopic model. The more small-signal models combined make the polytopic model more accurate, yet more complex to be calculated. Considering the complex process to combine the small-signal models in a linear way, a nonlinear model is more suitable for mapping the nonlinear relationships between the multi-operating-point impedance model and the measured data. The artificial neural network (ANN) provides a powerful nonlinear modeling method, which can be used to generate the complex nonlinear model by feeding the data. The ANN-based method features an automated training procedure with sufficient accuracy. A recurrent neural network (RNNs) based impedance measurement technique is reported for the power electronic systems [7], where the impedance is calculated by the trained RNN. Nevertheless, this method can only generate the impedance at a specific operating point.

This letter proposes an ANN-based impedance identification method to develop an impedance model that can cover multiple operating points. The impedance measurement method in the *dq*-frame is adopted first to obtain the impedance data of VSIs. Then, the measured data on a given set of operating points are used to train the ANN, in order to identify the impedance at the unmeasured operating points. Comparisons of the ANN-based identification against the analytical model are provided, which confirm the effectiveness of the proposed method.

II. ANN-Based Impedance Identification

A. ANN-Based Impedance Identification Framework

ANN is a nonlinear mathematical model that mimics the structure and function of a biological neural network, which can directly map the data to the model.

Fig. 1 illustrates a general framework of applying the ANN to identify impedance profiles of VSC at multiple operating points. The framework is organized with three levels, which are 1) the concept level, 2) the mapping level, and 3) the supporting level.

The concept level is composed of three conceptual steps in the machine learning algorithm, including the data-sourcing, the model generation, and the model verification.

The mapping level maps the machine-learning concepts to the physical domain of the impedance identification. First, in the data-sourcing step, the measured data, which can reflect the operating-point-dependent characteristic of the impedance, is obtained by the impedance measurement. The parameter range and interval of sweeping need to be defined at the beginning of the measurement, and then the commonly used *dq*-impedance measurement technique is executed to obtain the impedance data. As the impedance model of VSI can be changed with the operating point, a multi-operating-point impedance model will be established in this letter. Therefore, the parameters of operating point (V_d, V_q, I_d, I_q) are used as inputs to relate the impedance model with different operating points, while the

This article has been accepted for publication in a future issue of this journal, but has not been fully edited. Content may change prior to final publication. Citation information: DOI 10.1109/TPEL.2020.3012136, IEEE Transactions on Power Electronics

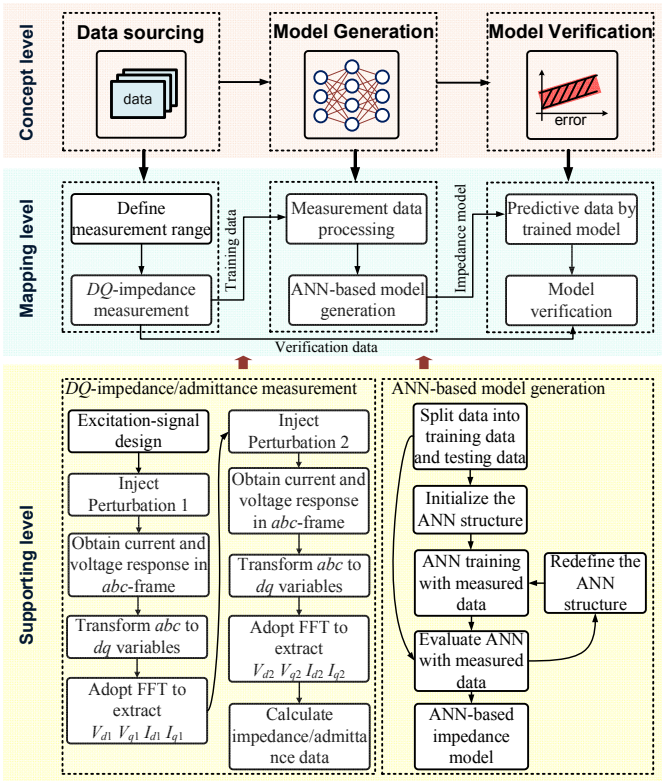

Fig. 1. General framework of the ANN-based impedance identification.

frequency f_p is also used as the input to reflect the frequency-dependent feature of the impedance model. The magnitude and the phase of impedance in the *dq*-frame are selected as the outputs. Thus, the measurement and calculation need to be repeated by changing the operating point of the inverter and the frequency of perturbation. After the impedance measurement at pre-defined operating points, the dataset is established. The measured dataset is then split into two parts, one is used for training the ANN, and the other for verifying the generated ANN model. The ANN-based model generation technique is next executed to generate a multi-operating-point impedance model that can identify the VSI impedance with the continuous changes of operating points. Prior to using the generated ANN model, the model accuracy is verified by comparing it with the measured data which are not used in model training.

The supporting level provides the detailed procedures of two techniques used to support the mapping level, which are the *dq*-impedance/*admittance* measurement technique and the ANN-based model generation technique. More detailed principles of these two techniques are explained in the next two parts.

B. DQ-Impedance/Admittance Measurement

Fig. 2 shows the admittance measurement diagram of grid-connected VSI with the PLL, the dc-link voltage control loop, and the current control loop. The perturbation is injected into the VSI, and by extracting the response at PCC, the output admittance of VSI can be obtained. $\mathbf{Y_{dq}}$ is a two by two admittance matrix.

The flowchart of measuring the VSI impedance/admittance in the *dq*-frame is illustrated in Fig. 1, which consists of

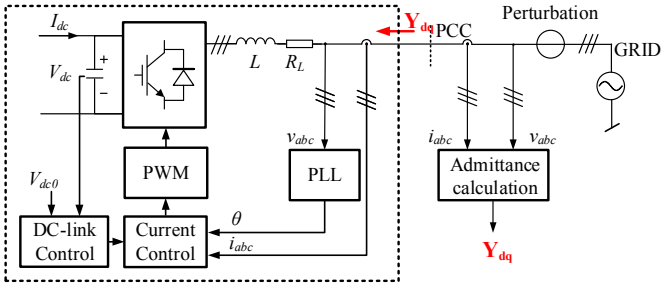

Fig. 2. A general diagram of *dq*-frame admittance measurement.

excitation-signal design, perturbation injection, data processing, and impedance/admittance calculation.

Before the measurement, the excitation signals need to be designed. The single-frequency injection is adopted to measure the admittance, considering the dynamic effect of PLL and dc-link [8]. The magnitude of this excitation signal has to be appropriately designed to extract the converter dynamics [9]. The magnitude of the excitation should neither be too large to change the operating point of the system, nor too small to be interfered by measurement noise. In general, the magnitude of the excitation signal is chosen between 5% and 10% of steady-state values [10], [11].

The next step is to inject the perturbation into the system and obtain the voltage and current response of the converter at PCC. Then the measured output current and voltage of the converter are transformed into the *dq*-frame. By applying the fast Fourier transform (FFT) to transformed variables, the magnitude and phase information for each voltage and current at the injected frequency can be extracted. To acquire the four entries of the admittance matrix $\mathbf{Y_{dq}}$ shown in Fig. 1, two linearly independent perturbations are applied [8], [12]. Based on the extracted magnitude and phase information, the *dq*-frame VSI admittance $\mathbf{Y_{dq}}$ can be derived as

$$\mathbf{Y_{dq}} = \begin{bmatrix} Y_{dd} & Y_{dq} \\ Y_{qd} & Y_{qq} \end{bmatrix} = \begin{bmatrix} I_{d1} & I_{d2} \\ I_{q1} & I_{q2} \end{bmatrix} \begin{bmatrix} V_{d1} & V_{d2} \\ V_{q1} & V_{q2} \end{bmatrix}^{-1} \quad (1)$$

C. ANN-Based Model Generation

The aim of the ANN-based model generation step is to obtain the multi-operating-point impedance model with the measured dataset and the ANN training technique. This step is split into two parts, i.e. the model initialization and the model training, which are elaborated as follows:

1) Model Initialization

Numerous types of ANN structures have been reported in the literature [13]. The choice of network structure depends on the

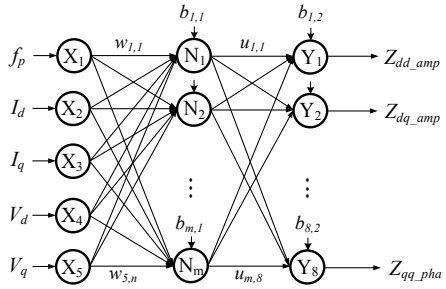

Fig. 3. Structure diagram of the ANN.

nature of the physical relationships of the trained data and the type of training task. The impedance identification is a regression task that generates the model from the measured data. The relationship between the output and input of the multi-operating-point impedance model is static. Hence, the feedforward ANN is selected in this letter.

The next step is to initialize the ANN structure, where the number of hidden layers and the neurons in each layer needs to be initialized. As the multi-operating-point impedance is defined as a five-input eight-output model, there are five neurons in the input layer and eight neurons in the output layer. Further, as the input-output relationship of the multi-operating-point impedance model is continuous, the single hidden layer is sufficient to solve the impedance identification application in this letter as one hidden layer is able to approximate any function that contains a continuous mapping from one finite space to another [14]. Yet the number of neurons in the hidden layer is selected by trial-and-error.

Therefore, a three-layer feedforward ANN is established. As shown in Fig. 3, the ANN contains an input layer, an output layer, and a hidden layer. In the hidden layer and output layer, each neuron is a processing unit, which first calculates their inputs by multiplying outputs of all neurons in the upper layer x with the given weights w, and then adds them together with the bias b. The result is next processed through the nonlinear function that is named as the activation function. In the hidden layer, the sigmoid function is selected as the activation function [15], since a shallow three-layer feedforward ANN is selected in this work. Therefore, the output of neurons in hidden layers is given as follows:

$$n_j = S\left[\sum_{i=1}^{5}\left(w_{i,j}\cdot x_i\right)+b_{j,1}\right], j=1,...,m \tag{2}$$

In the output layer, the activation function in the impedance identification is the linear function as the outputs are unbounded. Thus, the output of neurons in hidden layers is given as follows:

$$y_j = \sum_{i=1}^{m}\left(w_{i,j}\cdot x_i\right)+b_{j,2}, j=1,...,8 \tag{3}$$

2) Model Training

The process that generates the model with the data is named as the model training, which determines the accuracy of the resulted model. The purpose of the ANN model training in the impedance identification is to generate the multi-operating-point impedance model of the VSI with the measured operating point and impedance data. Prior to training, the training data used in model training step are split into two parts, 75% of the data is used for the ANN training, while the rest 25% is used for performance testing during the training process.

The next step is to train the model based on the initialized ANN structure. The back-propagation algorithm with the mean squared error (MSE) loss function between the ANN output and measured impedance data are used to train the ANN model. A stochastic gradient descent (SGD) algorithm is performed in mini-batches with multiple epochs to improve the learning convergence [16]. The MSE loss function is used as a default metric for evaluating the performance of regression algorithms, which is given as follows:

$$MSE = \frac{1}{N}\sum_{n=1}^{N}\sum_{d=1}^{D}\left(\hat{X}_n^d\left(\boldsymbol{w}^l,\boldsymbol{b}^l\right)-X_n^d\right)^2 \tag{4}$$

where $\hat{X}_n^d\left(\boldsymbol{w}^l,\boldsymbol{b}^l\right)$ and X_n^d denote the d-th ANN output and measured impedance data at the sample index n, respectively, N represents the mini-batch size, D is the size of the ANN output vector, and ($\boldsymbol{w}^l$, $\boldsymbol{b}^l$) denotes the weights and bias parameters to be learned at the l-th layer.

The random initialization of the weights and bias parameters based on the Gaussian distribution shows more probability and is suitable for the unknown or highly nonlinear relationship [17]. The training process is to minimize the MSE loss function by optimizing the weights and bias parameters. The updated procedure with a learning rate λ, can be computed as follows,

$$\left(\boldsymbol{w}_k^l,\boldsymbol{b}_k^l\right)=\left(\boldsymbol{w}_{k-1}^l,\boldsymbol{b}_{k-1}^l\right)-\lambda\frac{\partial MSE}{\partial\left(\boldsymbol{w}_{k-1}^l,\boldsymbol{b}_{k-1}^l\right)} \tag{5}$$

After the training, the generated model is evaluated by the coefficient of determination (R^2) to show the performance of training, which is given by

$$R^2 = 1-\sum_i\left(y_i-f_i\right)^2/\sum_i\left(y_i-\bar{y}\right)^2 \tag{6}$$

where y_i denotes the training data, $\bar{y}$ denotes the average value of y_i. f_i denotes the corresponding generated data by the trained model. If the calculated R^2 is smaller than 0.98, the number of neurons in each hidden layer needs to be redefined.

III. Case Study and Validation

To verify the proposed method, the method is applied to identify a grid-connected VSI shown in Fig. 2 with the PLL, the dc-link voltage control loop, and the current control loop. To simplify the measurement, only the variation of d-axis current in the dq-frame is taken into consideration.

The parameters of the inverter are shown in Table I. In this letter, the data are extracted by the analytical model, which is validated by the field measurements [8]. The dataset is split into two parts, i.e. training dataset and verification dataset. In the training dataset, the frequency f_p was swept from 1 Hz to 100 Hz with an interval of 1 Hz, whereas the operating current I_d was swept from 2.16 A to 9.84 A with an interval of 0.16 A. To make the result easily visible, the results are separated into Y_{dd}, Y_{dq}, Y_{qd}, Y_{qq}. The obtained output admittance dataset for training is shown in Fig. 4. Then the obtained dataset is fed into the initialized ANN. After the training process, the operating-point-dependent admittance model Y_{ANN} is generated as shown in Fig. 5.

To verify the accuracy of the proposed method, the generated ANN-based model needs to be compared with the verification dataset that is not used in training with the corresponding frequency f_{p_v} and operating current I_{d_v}. In the verification dataset, the frequency f_{p_v} was swept from 1 Hz to 100 Hz with an interval of 0.1 Hz, whereas the operating current I_{d_v} was swept from 2.16 A to 9.84 A with an interval of 0.04 A.

The corresponding errors between the verification data and the generated model are shown in Fig. 6, where the errors become large when the data used in training is sparse, yet the

This article has been accepted for publication in a future issue of this journal, but has not been fully edited. Content may change prior to final publication. Citation information: DOI 10.1109/TPEL.2020.3012136, IEEE Transactions on Power Electronics

TABLE I. INVETRTER PAERMETERS

Symbol	Description	Value
V_{dc0}	Inverter input dc voltage reference	730 V
V_d	D channel grid voltage	250V
V_q	Q channel grid voltage	0 V
I_q	Q channel output current	0 A
f_{sw}	Switching frequency	10 kHz
f_0	Line frequency	50 Hz
L_f	Inductance of inverter output inductor	3 mH
C_{dc}	DC capacitor	1000 μF
K_{p_dc}	Proportional gain of dc voltage controller	0.1
K_{i_dc}	Integral gain of dc voltage controller	10
K_{p_i}	Proportional gain of current controller	7.85
K_{i_i}	Integral gain of current controller	2741.5
K_{p_pll}	Proportional gain of inverter PLL	0.56
K_{i_pll}	Integral gain of inverter PLL	80.75

largest error is only 1 % of the verification data. Hence, the proposed ANN-based impedance identification method can accurately model the VSI considering the operating point variation.

IV. CONCLUSION

This letter has discussed an ANN-based impedance identification method to consider the operating-point variation in the VSI impedance model. A framework for illustrating the use of ANN for the impedance estimation has been introduced. The case study has demonstrated the effectiveness of the method.

REFERENCES

[1] X. Wang and F. Blaabjerg, "Harmonic Stability in Power Electronic-Based Power Systems: Concept, Modeling, and Analysis," *IEEE Trans. Smart Grid*, vol. 10, no. 3, pp. 2858–2870, May 2019.

[2] L. Harnefors, M. Bongiorno, and S. Lundberg, "Input-admittance calculation and shaping for controlled voltage-source converters," *IEEE Trans. Ind. Electron.*, vol. 54, no. 6, pp. 3323–3334, Dec. 2007.

[3] X. Wang, "Unified Impedance Model of Grid-Connected Voltage-Source Converters," *IEEE Trans. Power Electron.*, vol. 33, no. 2, pp. 1775–1787, Feb. 2018.

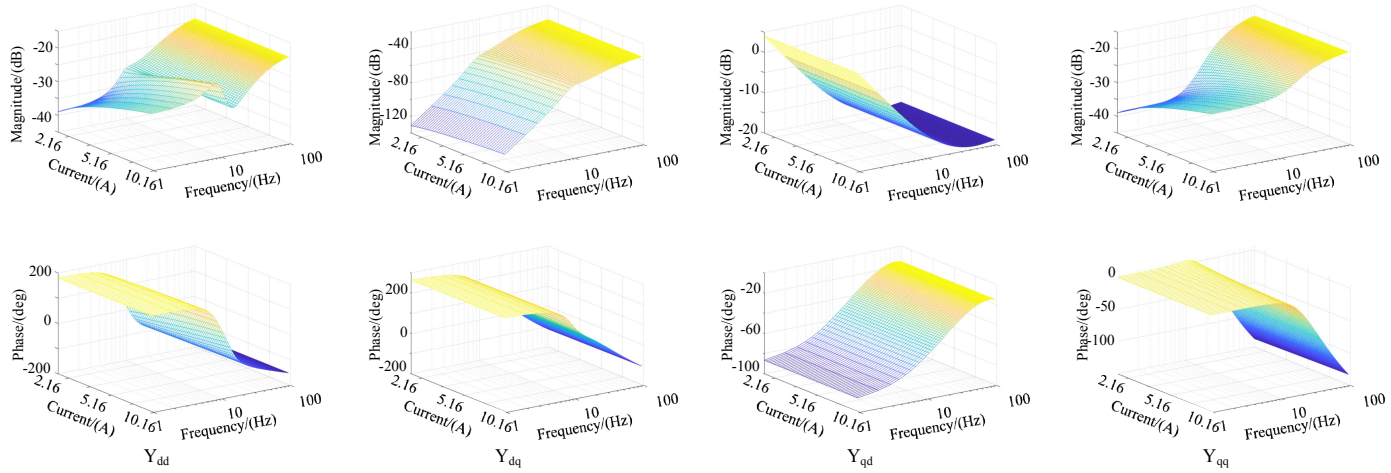

Fig. 4. Output admittance dataset of VSI used for training.

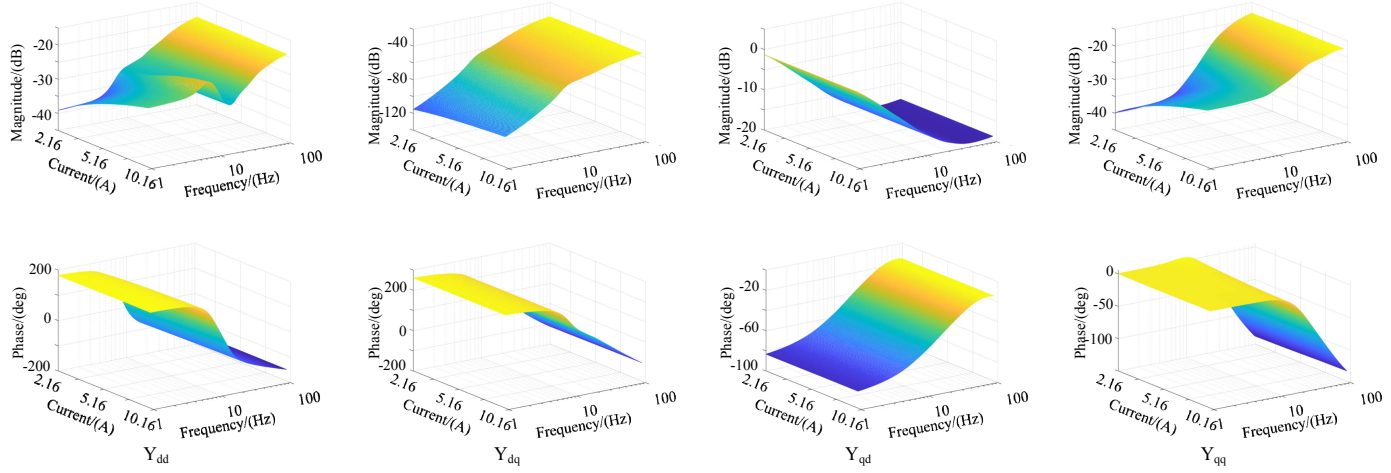

Fig. 5. Generated multi-operating-point admittance model of VSI.

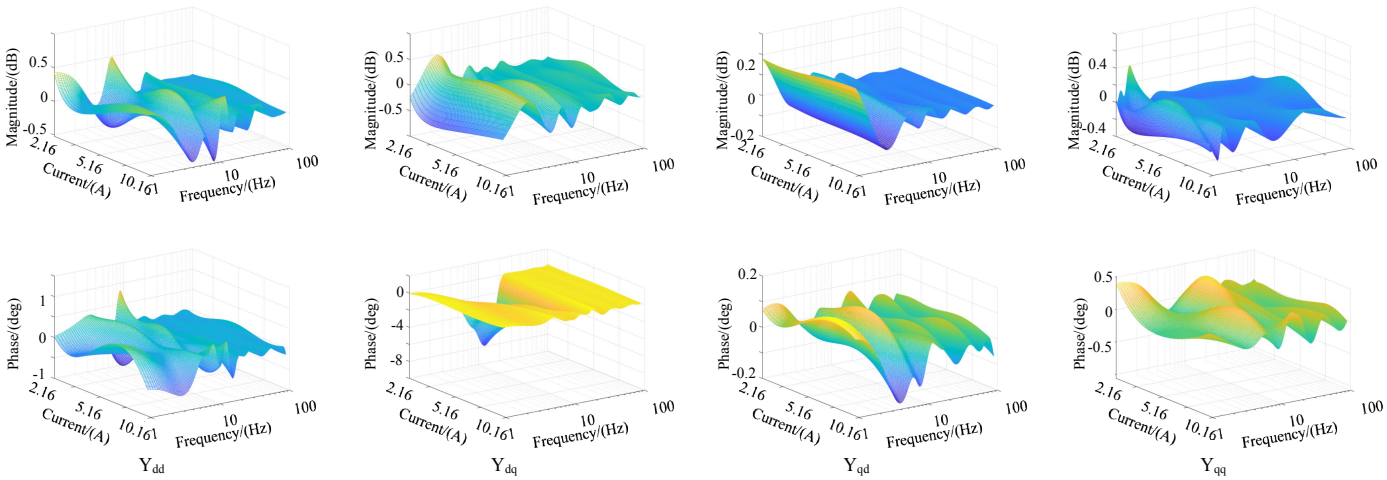

Fig. 6. Corresponding errors between generated multi-operating-point admittance model and verification data.

[4] S. Shah et al., "Large-Signal Impedance-Based Modeling and Mitigation of Resonance of Converter-Grid Systems," *IEEE Trans. Sustain. Energy*, vol. 10, no. 3, pp. 1439–1449, July 2019.

[5] V. Valdivia et al., "Simple Modeling and Identification Procedures for 'Black-Box' Behavioral Modeling of Power Converters Based on Transient Response Analysis," *IEEE Trans. Power Electron*., vol. 24, no. 12, pp. 2776–2790, Dec. 2009.

[6] A. Francés, R. Asensi, and J. Uceda, "Blackbox Polytopic Model With Dynamic Weighting Functions for DC-DC Converters," *IEEE Access*, vol. 7, pp. 160263–160273, Nov. 2019.

[7] P. Xiao, G. K. Venayagamoorthy, K. A. Corzine, and J. Huang, "Recurrent neural networks based impedance measurement technique for power electronic systems," IEEE Trans. Power Electron., vol. 25, no. 2, pp. 382–390, Feb. 2010.

[8] H. Gong, D. Yang and X. Wang, "Impact of Nonlinear Dynamics on Converter DQ Impedance Measurement," in *Proc. Control and Modeling for Power Electronics (COMPEL)*, June 2019, pp. 1-6.

[9] B. Miao, R. Zane and D. Maksimovic, "System identification of power converters with digital control through cross-correlation methods," *IEEE Trans. Power Electron*., vol. 20, no. 5, pp. 1093-1099, Sept. 2005.

[10] A. Riccobono, M. Mirz, and A. Monti, "Noninvasive online parametric identification of three-phase AC power impedances to assess the stability of grid-tied power electronic inverters in LV networks," *IEEE J. Emerg.Sel. Top. Power Electron*., vol. 6, no. 2, pp. 629-647, June 2018.

[11] A. Riccobono, E. Liegmann, M. Pau, F. Ponci and A. Monti, "Online parametric identification of power impedances to improve stability and accuracy of power hardware-in-the-loop simulations," *IEEE Trans. Instrum. Meas.*, vol. 66, no. 9, pp. 2247-2257, Sept. 2017.

[12] Z. Shen, M.Jaksic, B.Zhou, P.Mattavelli, J.Verhulst, M.Belkhayat, "Analysis of Phase Locked Loop (PLL) influence on DQ impedance measurement in three-phase AC systems," in *Proc. Appl. Power Electron. Conf. Expo*., Mar. 2013, pp. 939–945.

[13] J. Schmidhuber, "Deep learning in neural networks: An overview," *Neural Netw*., vol. 61, pp. 85–117, Jan. 2015.

[14] R. P. Lippmann, "An introduction to computing with neural nets," *IEEE ASSP Magazine*, pp. 3-22, Apr. 1987.

[15] P. Ramachandran, B. Zoph, and Q. V. Le, "Searching for activation functions," 2017, *arXiv: 1710.05941*. [Online]. Available: https://arxiv.org/abs/1710.05941.

[16] L. Bottou, "Large-scale machine learning with stochastic gradient descent," in *Proc. 19th Int. Conf. Comput. Statist*., pp. 177–186, Sept. 2010.

[17] S. S. Du, X. Zhai, B. Poczos, and A. Singh, "Gradient descent provably optimizes over-parameterized neural networks," 2018, *arXiv: 1810.02054*. [Online]. Available: https://arxiv.org/abs/1810.02054.